Stochastic model for short-term balancing of supply and consumption of electricity

Jeanne Andersen* Michal Kaut† Asgeir Tomasgard‡

April 10, 2015

In this paper, we present a two-stage stochastic mixed integer model for the intra-hour balancing problem faced by system operators in electricity systems with large penetration of wind power production. Since wind power is non-controllable and intermittent, it is difficult to predict wind power production. Wind power prediction errors directly impact the balance between supply and demand of electricity. Therefore, it is of utmost importance for the system operators to understand and investigate these errors and plan accordingly when balancing the transmission system. In this model, we capture the uncertainty in wind power production forecasts by generating scenarios for the prediction errors. We apply the model on realistic Danish system data. We compare the stochastic solution and the deterministic solution to the solution of perfect foresight, and we find that wind power prediction errors entail huge balancing costs. Furthermore, we see that the stochastic solution incorporate a buffer when activating manual reserves compared to the deterministic solution. The buffer results in higher expected cost, but the actual cost incurred is lower compared to the deterministic solution in most of the cases.

1. Introduction

With existing technology, electricity cannot be stored large-scale in any feasible way. Since it cannot be stored, the electricity has to be produced in the same second as it is consumed. It is the responsibility of the system operator (SO) to balance the system such that supply always equals consumption. With an increasing penetration of fluctuating renewable energy sources such as solar and wind power, the supply of electricity becomes highly uncertain. However, fluctuations can be met by planned conventional electricity production from thermal plants

*CORAL, Department of Economics and Business, Aarhus University, Aarhus, Denmark. jeand@econ.au.dk
†SINTEF Technology and Society, Applied Economics, Trondheim, Norway. michal.kaut@sintef.no
‡Department of Industrial Economics and Technology Management, NTNU, Trondheim, Norway. asgeir.tomasgard@iot.ntnu.no

but only to the extent that the power from the fluctuating energy sources are forecasted accurately. When there is a prediction error, the excess or shortage of electricity must be handled through reserved power capacity on plants dedicated to this purpose. Thereby, the security of the electricity system depends on accessibility of reserved power capacity for increased or reduced electricity production.

The purpose of this paper is to develop a two-stage stochastic mixed integer model that can be used to analyse how to balance supply and demand of electricity within the hour seen from an SO's perspective. The model is supposed to be used for analysing purposes, e.g. how different ramping patterns between flow levels from transmission lines effect the system balance or how different balancing policies result in different balancing costs.

Wind power production is one of the most promising large-scale renewables in Northern Europe to replace some of the conventional supply. Therefore, in this paper, we look at an electricity system with a large amount of installed wind capacity, and the stochasticity of the model lies in the uncertainty in the wind power production. In order to capture the uncertainty, we make scenarios for the wind power prediction error. The model is an extension of the deterministic Nordic balancing model presented in Andersen et al. (2014). A stochastic model can capture the uncertainty of wind and thereby give a more precise picture of intra-hour challenges related to wind power production.

When balancing an electricity system in the case of updated new information (e.g. new wind power forecasts), the SO can use two different strategies. Either they can be *proactive* and re-dispatch generating units by activating or deactivating reserved capacity before real-time operation, or they can wait until the imbalances occur and then re-dispatch the generating units by activating or deactivating reserved capacity at the time the imbalances occur. If the SO is proactive and able to forecast expected imbalances with high accuracy, smaller imbalances will occur real-time. This way *balancing costs* can be reduced since activation of reserved capacity is often cheaper the longer activation time, the generating unit has. We will refer to re-dispatching generating units before real-time operation as activating *manual reserves* and real-time activation or deactivation of reserved power capacity as activating *automatic reserves*.

In this paper, we assume that the SO is proactive and that the already committed units in the day-ahead market make their capacity for either additional or reduced electricity supply available to the SO. We consider balancing close to real-time operation when commitment schedules, production plans for generating units, and forecasts for consumption and wind power production have been made and converted to an intra-hour time resolution. An example on how to convert hourly schedules and forecasts into an intra-hour time resolution can be seen in Andersen et al. (2014). On the basis of the intra-hour schedules and forecasts, the presented model re-dispatches the generating units before real-time operation in order to minimise balancing cost. It is assumed that the unit commitment schedule is fixed, and therefore our model only considers re-dispatch of already committed units.

Intra-hour balancing is closely related to the unit commitment (UC) problem, where start-ups, shut-downs, and production levels for the generating units are decided upon, usually with an hourly resolution. Stochastic UC models with scenarios for wind power production have been studied intensively in literature. Where some have made scenarios for the wind power production (e.g. Pappala et al. (2009)), others have made scenarios for the wind speed and afterwards converted wind speed to power (e.g. Papavasiliou and Oren (2013)). However, UC

models with an hourly resolution do not capture fluctuations of wind power production within the hour. To get the detailed information about the system within the hour, intra-hour models can be used. Even though some intra-hour models have focused on uncertainty in wind power production (e.g. Lindgren and Söder (2008); Ela and O'Malley (2012)), only few have looked at intra-hour stochastic models for the balancing problem faced by SOs (e.g. Delikaraoglou et al. (2014)). However, to the best of our knowledge, no study has a stochastic balancing model as detailed as presented in this paper where technical ramping restrictions are included.

When making scenarios for wind power production in general, the emphasis has mainly been on wind power forecasts and not so much on the study of wind power prediction errors. Even though the wind power prediction error is a result of the forecast, understanding the nature of the error is extremely important for the SO since the error is one of the major sources for imbalances in an electricity system with high penetration of wind power. Studies (e.g. Doherty and O'Malley (2005); Menemenlis et al. (2012)) have been carried out on how the wind power prediction error affects the need for reserves and Menemenlis et al. (2012) show the importance of the wind power prediction error classification when determining the level of reserves.

It has often been assumed that the wind power prediction error can be described by a Gaussian distribution (e.g. see Doherty and O'Malley (2005); Bouffard and Galiana (2008)). However, as Bludszuweit et al. (2008) and Hodge and Milligan (2011) point out, the error distribution depends on the forecasting horizon and method. The prediction error also depends on the forecast being for a single wind turbine or for aggregated wind farms (Tewari et al. (2011)). The prediction errors from forecasts with a long forecast horizon and aggregated wind farms may be described by the Gaussian or Normal distribution where the distribution of prediction errors from forecasts with a shorter time horizon is heavy-tailed with variable kurtosis and hence cannot be described by the Gaussian distribution (Bludszuweit et al. (2008); Hodge and Milligan (2011)). To capture the heavy-tailed nature of the distribution of the short-term error, Bludszuweit et al. (2008) suggest the Beta distribution. Other distributions such as a Lévy alpha-stable distribution (Bruninx and Delarue (2014)), the Cauchy distribution (Hodge and Milligan (2011)), and the Gamma distribution (Menemenlis et al. (2012)) have also been suggested. Lately, Wu et al. (2014) proposed a mixed distribution based on the Laplace and Normal distribution to approximate the wind power prediction error. Lange (2005) takes another approach; assuming that the wind speed error to be Gaussian, they transform the wind speed error into wind power errors by Taylor-expansions.

In all of the before mentioned studies; the description of the correlation of error in time is absent. Pinson et al. (2009) address this problem by converting uniformly distributed series of wind power prediction errors to a multivariate Gaussian random variable, where the interdependence structure can be described by a unique covariance matrix. This matrix is recursively estimated in order to account for the variations in the characteristics of the errors. Ma et al. (2013) expand the work done in Pinson et al. (2009) by including empirical distributions of the prediction errors. In Litong-Palima et al. (2012), they account for the correlation of prediction errors in time by generating day-ahead and hour-ahead wind power prediction errors on a five minute resolution by an ARMA(1,1) process, where the independent random variable is assumed to follow a Gaussian distribution. The detailed resolution is obtained by using linear interpolation between the hourly wind power prediction errors. Söder (2004) and Weber et al. (2009), on the other hand, assume that the wind speed prediction error can be described with an

ARMA(1,1) process, where the independent random variable is assumed to follow a Gaussian distribution. They use a multidimensional ARMA(1,1) model to capture the positive correlation of the wind speed prediction error between different sites. In Matevosyan and Söder (2006), they use the approach described in Söder (2004) to generate different outcomes for the wind speed error and convert it to scenarios for the wind power production. The scenarios are used in a stochastic model which generates optimal wind power production bids from the wind farm owners to the power market.

In this paper, we use a different approach. We generate the outcomes of the error term using a copula-based heuristic from Kaut (2014). In particular, we use a nonparametric version of the method that attempts to replicate the distribution of the historical data, so we avoid extra assumptions about the underlying distributions.

To summarise, our contribution to the existing literature is twofold:

- We develop a stochastic two-stage model for the intra-hour balancing problem. The model can be used for analysing electricity systems operations within the hour, such as intra-hour variations, the effect of ramping patterns, or the minimum level of automatic reserves. With minor modifications, the model can be used in operational planning.
- We show how to make scenarios for the short-term wind power production by generating scenarios for the wind power prediction error by a copula-based heuristic.

The rest of the paper is divided into sections as follows. In the following section, we describe the stochastic balancing problem and present our model. Then, we describe our scenario-generation procedure in in Section 3. Finally, we apply our model to a Danish case in Section 4.

2. The stochastic balancing model

The balancing problem described in this paper involves two sets of decisions. First, the manual reserves are activated based on expected imbalances, and afterwards, when the uncertain wind power prediction errors are revealed, the automatic reserves are activated. This can be seen as a two-stage stochastic model, where the SO decides on the level of manual reserves that have to be activated in the first stage, and in the second stage, the automatic reserves are activated based on the actual imbalances caused by the wind power prediction errors.

In addition to the deterministic model presented in Andersen et al. (2014), we have in this model included uncertainty in the wind power forecast and made a simplification in the activation of manual reserves. However, for the readability and completeness of the model, we include all the notation and explanation of the first stage constraints, even though some of it is as presented in Andersen et al. (2014).

2.1. Notation

We start out by discretising the time horizon, $[0, T]$, of the stochastic model into τ-minute intervals $]\tau(t-1), \tau t]$, $t = 1, \ldots, T/\tau$. Let $\mathcal{T} = \{0, \ldots, T/\tau\}$. The time periods are further grouped into Λ groups, such that each group λ, where $1 \leq \lambda \leq \Lambda$, has $|\mathcal{T}_\lambda|$ time periods. Since we describe a two-stage model, we let $\Lambda = 2$, a group for each stage. $\mathcal{T}$ then consists of the

two subsets $\mathcal{T}_1$ and $\mathcal{T}_2$, where $\mathcal{T}_1 = \{0\}$ and $\mathcal{T}_2 = \{1, \ldots, T/\tau\}$. The first stage is assumed to be deterministic, so we have one stochastic stage $\mathcal{T}_2$ with T/τ stochastic periods.

The transmission grid is modelled as a network $(\mathcal{N}, \mathcal{A})$ with nodes $\mathcal{N} = \{1, \ldots, N\}$ and arcs $\mathcal{A} = \{a : a = (n, n'), n, n' \in \mathcal{N} : n < n'\}$ representing transmission lines. We denote by $\delta^{out}(n) = \{a : a = (n, n'), n' \in \mathcal{N}\}$ and $\delta^{in}(n) = \{a = (n', n), n' \in \mathcal{N}\}$ the sets of arcs either originating from or terminating in node n, respectively. For $a \in \mathcal{A}$, we let the capacity of transmission line a be $L_a^{\max}$. Moreover, we let the flow allocated day-ahead to line a in time interval t be L_{at}. If $a = (n, n')$ and $L_{at} > 0$ there is a net import from n to n'. If $L_{at} < 0$ there is a net export. We represent the intra-hour scheduled import determined by our model on the transmission line in the same time interval by the variable Δl_{at} using the same conventions regarding its sign. The allowed change in the flow on a transmission line between two time periods will be denoted by R_a.

The set of all conventional units is denoted by $\mathcal{I}$, the set of units online in time interval t is denoted $\mathcal{I}_t$, and the units located in node n by $\mathcal{I}_n$. For $i \in \mathcal{I}$, we denote the planned production day-ahead in time interval t by the parameter P_{it}, and the plant's minimum and maximum production limits by $P_i^{\min}$ and $P_i^{\max}$, respectively. The model will minimise expected imbalances by doing short-term production planning, and it decides, based on updated weather forecasts, to produce $P_{it} + \Delta p_{it}^+ - \Delta p_{it}^-$, instead of P_{it}. The first-stage decision variables $\Delta p_{it}^+ \geq 0$ and $\Delta p_{it}^- \geq 0$ represent the balancing power provided by intra-hour activation of manual reserves on the unit in the time interval. When doing short-term production planning, we must for each unit i and time interval t obey

$$P_i^{\min} \leq P_{it} + \Delta p_{it}^+ - \Delta p_{it}^- \leq P_i^{\max}.$$

However, in real time, there will still be imbalances that have to be dealt with using the automatic reserves. The extra produced or reduced power is illustrated by the second stage variables $q_{nts}^+ \geq 0$ and $q_{nts}^- \geq 0$, which represent the generation surplus or shortage in node n in scenario $s \in \mathcal{S}$ during time interval t. Note, that we do not have any limits on the production from automatic reserves. Firstly, there exist plants whose only purpose is to supply automatic reserves and hence are not included in the set $\mathcal{I}$. Secondly, by not restricting the second stage variables, we are guaranteed to always have a feasible solution to the problem. Hence, the model can indicate which level of automatic reserves that are needed in order to maintain a secure system.

We denote by C_i the variable generation cost of unit $i \in \mathcal{I}$. The late scheduling of the units close to real time operation incurs extra variable cost γC_i. Note, whereas activation of power generates a cost, deactivation of power results in cost savings from not producing. We therefore let $C_i^+ := (1 + \gamma)c_i$ and $C_i^- := (1 - \gamma)c_i$, with $\gamma \in [0, 1]$, be the costs of activated manual reserve power and savings from deactivated manual reserve power, respectively. The idea is to allow the costs and savings to reflect the additional stress imposed on the unit when using it for balancing purposes. Since P_{it} is already decided, we do not include its costs in the model. The costs of activating automatic reserves in node n are denoted by C_n^+ and C_n^-, where most likely $C_n^+ > \max_i C_i^+$ and $C_n^- < \min_i C_i^-$. In other words, it is likely that there is a higher cost for extra production and lower savings for production decrease in the case of automatic reserves compared to the manual reserves.

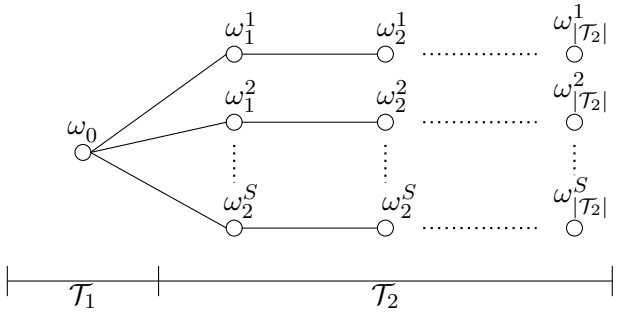

Figure 1: Scenario tree.

In order to keep track of the activated manual reserves, we let the variables g_{it}^+ and g_{it}^- be the amount of recently activated and deactivated power on unit i in time interval t, respectively. If new manual reserves are activated on a unit, it has to provide the committed level for at least τ^{res} time periods. If we activate or deactivate manual reserve power, we let the associated binary variables v_{it}^+ or v_{it}^- be one and zero otherwise. The amount of recently activated or deactivated manual reserve power has to be above the threshold value $G_i^{\min}$. Furthermore, we introduce the variables $g_{it}^{\text{ramp},+}$ and $g_{it}^{\text{ramp},-}$ to record the ramping power generated by a unit providing manual reserves, where $g_{it}^{\text{ramp},+}$ is related to activating power and $g_{it}^{\text{ramp},-}$ to deactivating power. How much the production level is allowed to change from one time period to another will be denoted by R_i^+ when the unit is ramping up, and by R_i^- when the unit is ramping down. A unit is only allowed to ramp $\tau^{\max}$ time periods before a new activation level, and $\tau^{\max}$ time periods after the activation period of τ^{res} time periods.

We assume that the demand is inflexible, meaning that the level of demand in each time period is maintained at the forecasted level. We denote by the parameter D_{nt} its value in node n in time interval t.

The uncertainty is modelled using scenarios $s \in \mathcal{S} = \{1, \ldots, S\}$ with probability Π^s and $\sum_{s\in\mathcal{S}} \Pi^s = 1$. The only stochastic parameter in the model is the wind power production ω_{nt}^s for $t \in \mathcal{T}_2$, with the first-stage deterministic values denoted by ω_{nt}, for $t \in \mathcal{T}_1$. This results in the scenario tree presented in Fig. 1, where we have omitted the node subscripts, i.e. all the values are vectors of size N.

2.2. Objective function

We schedule the activation of manual reserves Δp_{it}^+ and Δp_{it}^-, such as to cover any expected imbalances between supply and consumption. Occasionally, this may be technically infeasible, or it may be feasible only at very high costs, in which case imbalances are left to automatic reserves q_{nts}^+ and q_{nts}^-. Since the uncertainty in wind power is revealed after activation of manual reserves, the amount of automatic reserves depends on the realisation of the wind power prediction error, and hence, we have an outcome with a probability Π^s for each scenario. The optimal schedule is determined by a trade-off between the activation cost of manual and

automatic reserves. The objective is

$$\sum_{t\in\mathcal{T}_2}\Big(\sum_{i\in\mathcal{I}_t}(C_i^+\Delta p_{it}^+ - C_i^-\Delta p_{it}^-) + \sum_{s\in\mathcal{S}}\Pi^s\big(\sum_{n\in\mathcal{N}}(C_n^+ q_{nts}^+ - C_n^- q_{nts}^-)\big)\Big),$$

which is minimised subject to a number of constraints presented next.

2.3. Balancing constraint

The balancing constraint ensures system balance between supply and consumption. According to this constraint, if at any point in time scheduled production exceeds predicted consumption D_{nt} or vice versa, we experience generation surplus or shortage, which will be left to the automatic reserves q_{nts}^+ and $-q_{nts}^-$. We assume that it is always possible to provide the sufficient amount of automatic reserves. Production includes day-ahead planned generation on conventional units P_{it}, intra-hour activation of manual reserves Δp_{it}^+ and Δp_{it}^-, forecasted wind power production ω_{nt}^s, and finally day-ahead and intra-hour net import/export on the transmission lines $L_{at} + \Delta l_{at}$. Thus, we have that

$$\begin{aligned}&\sum_{i\in\mathcal{I}_t\cap\mathcal{I}_n}(P_{it} + \Delta p_{it}^+ - \Delta p_{it}^-) + \sum_{a\in\delta^{in}(n)}(L_{at} + \Delta l_{at})\\ &- \sum_{a\in\delta^{out}(n)}(L_{at} + \Delta l_{at}) + q_{nts}^+ - q_{nts}^- = D_{nt} - \omega_{nt}^s,\ \ n\in\mathcal{N}, t\in\mathcal{T}_2, s\in\mathcal{S}.\end{aligned} \tag{1}$$

2.4. Limits on re-dispatch variables

Transmission flow is restricted by the available line capacity. In particular, intra-hour import Δl_{at} on the transmission lines is bounded above by the line capacity $L_a^{\max}$ minus the capacity allocated day-ahead L_{at}. Thus, we have that

$$-(L_a^{\max} - L_{at}) \le \Delta l_{at} \le L_a^{\max} - L_{at},\ \ a\in\mathcal{A}, t\in\mathcal{T}_2.$$

Activation of manual reserve power is bounded above by the maximum capacity $P_i^{\max}$ that has not already been dispatched day-ahead P_{it}, whereas deactivation is bounded by the dispatched capacity in excess of the minimum capacity $P_i^{\min}$. Formally,

$$\begin{aligned}\Delta p_{it}^+ &\le P_i^{\max} - P_{it},\ \ i\in\mathcal{I}_t, t\in\mathcal{T}_2,\\ \Delta p_{it}^- &\le P_{it} - P_i^{\min},\ \ i\in\mathcal{I}_t, t\in\mathcal{T}_2.\end{aligned}$$

2.5. New generation level of a unit

We require the minimum threshold value $G_i^{\min}$ to be obtained when activating manual reserves. The threshold value is included in order to make it profitable for the unit to change the production level. Manual reserves are activated when v_{it}^+ (v_{it}^-) is equal to one at the level g_{it}^+ (g_{it}^-).

$$G_i^{\min} v_{it}^+ \le g_{it}^+ \le M v_{it}^+,\ \ i\in\mathcal{I}_t, t\in\mathcal{T}_2, \tag{2}$$

$$G_i^{\min} v_{it}^- \le g_{it}^- \le M v_{it}^-,\ \ i\in\mathcal{I}_t, t\in\mathcal{T}_2, \tag{3}$$

where M is a sufficiently large number, e.g. $P_i^{\max}$.

It is only allowed to either activate or deactivate manual reserve power on the same unit in one time interval, hence,

$$v_{it}^{+} + v_{it}^{-} \leq 1, \;\; i \in \mathcal{I}_t, t \in \mathcal{T}_2. \tag{4}$$

Additional levels of reserves may be activated on the same unit at a given point in time. This we refer to as activating new reserves. The amount of manual reserves a unit provides at a given point in time can be calculated by

$$\Delta p_{it}^{+} = \sum_{t'=\max\{1,t-\tau^{\text{res}}+1\}}^{t} g_{it'}^{+} + g_{it}^{\text{ramp},+}, \;\; i \in \mathcal{I}_t, t \in \mathcal{T}_2, \tag{5}$$

$$\Delta p_{it}^{-} = \sum_{t'=\max\{1,t-\tau^{\text{res}}+1\}}^{t} g_{it'}^{-} + g_{it}^{\text{ramp},-}, \;\; i \in \mathcal{I}_t, t \in \mathcal{T}_2, \tag{6}$$

where τ^{res} is the fixed time from time t and forward, for which the activated reserves have to provide the level $g_{it'}^{+}$ ($g_{it'}^{-}$) of power. The actual manual reserves provided by a unit are the activation level plus the ramping power $g_{it}^{\text{ramp},+}$ ($g_{it}^{\text{ramp},-}$) it provides in order to reach the agreed level.

2.6. Ramping

Ramping constraints on the transmission lines are restrictions on the change in allocated transmission flow from one time interval to another and apply to net import. In order to record the change from one time interval to another, we need to include both the day-ahead agreed flow amount L_{at} and the variation decided by our model Δl_{at} from the time intervals. Thus,

$$\begin{aligned} -R_a - L_{a(t+1)} + L_{at} \leq \Delta l_{a(t+1)} - \Delta l_{at} \leq R_a - L_{a(t+1)} + L_{at}, \\ a \in \mathcal{A}, t \in \mathcal{T}_2 : t \leq |\mathcal{T}_2| - 1. \end{aligned}$$

It is allowed to change the flow on the transmission line by R_a between two time intervals.

For the generating units, we include detailed ramping restrictions where the change in day-ahead planned production P_{it} is taken into account.

$$\begin{aligned} -(R_i^{-} + P_{i(t+1)} - P_{it}) \leq \Delta p_{i(t+1)}^{+} - \Delta p_{it}^{+} \leq (R_i^{+} - P_{i(t+1)} + P_{it}), \\ i \in \mathcal{I}_t, t \in \mathcal{T}_2 : t \leq |\mathcal{T}_2| - 1, \end{aligned} \tag{7}$$

$$\begin{aligned} -(R_i^{+} - P_{i(t+1)} + P_{it}) \leq \Delta p_{i(t+1)}^{-} - \Delta p_{it}^{-} \leq (R_i^{-} + P_{i(t+1)} - P_{it}), \\ i \in \mathcal{I}_t, t \in \mathcal{T}_2 : t \leq |\mathcal{T}_2| - 1. \end{aligned} \tag{8}$$

The allowed ramping speed between two time intervals is R^{+} for activation of power, where it is R^{-} for deactivation.

Generating units can only ramp towards a new level in $\tau^{\max}$ time periods before the amount of activated reserves has to be fully activated and in the $\tau^{\max}$ time periods after the activation period of τ^{res} time periods.

$$g_{it}^{\text{ramp},+} \leq M \sum_{\min\{T,t+1\}}^{\min\{T,t+\tau^{\max}\}} v_{it'}^{+} + M \sum_{\max\{1,t-\tau^{\max}-\tau^{\text{res}}+1\}}^{\max\{1,t-\tau^{\text{res}}\}} v_{it'}^{+}, \quad i \in \mathcal{I}_t, t \in \mathcal{T}_2, \tag{9}$$

$$g_{it}^{\text{ramp},-} \leq M \sum_{\min\{T,t+1\}}^{\min\{T,t+\tau^{\max}\}} v_{it'}^{-} + M \sum_{\max\{1,t-\tau^{\max}-\tau^{\text{res}}+1\}}^{\max\{1,t-\tau^{\text{res}}\}} v_{it'}^{-}, \quad i \in \mathcal{I}_t, t \in \mathcal{T}_2, \tag{10}$$

where M is a sufficiently large number, e.g. $P_i^{\max}$. If $v_{it'}^{+}$ ($v_{it'}^{-}$) is equal to 1 in the constraint, it indicates that an activation (deactivation) of manual reserve power has occurred at time t', and thereby it is possible for the unit to ramp by activating (deactivating) $g_{it}^{\text{ramp},+}$ ($g_{it}^{\text{ramp},-}$) power in the $\tau^{\max}$ time periods before time t' and after time $t' + \tau^{\text{res}}$.

If new reserves are activated, and thereby a new level of production is committed on a unit in one time period, ramping is not allowed in the same period on the same unit. Hence,

$$g_{it}^{\text{ramp},+} \leq M(1 - v_{it}^{+}), \quad i \in \mathcal{I}_t, t \in \mathcal{T}_2, \tag{11}$$

$$g_{it}^{\text{ramp},-} \leq M(1 - v_{it'}^{-}), \quad i \in \mathcal{I}_t, t \in \mathcal{T}_2, \tag{12}$$

where M is a sufficiently large number, e.g. $P_i^{\max}$.

Since ramping in optimisation can adapt to the imbalances, we restrict the ramping to a linear pattern.

$$g_{it}^{\text{ramp},+} = \frac{\Delta p_{i(t-1)}^{+} + \Delta p_{i(t+1)}^{+}}{2}, \quad i \in \mathcal{I}_t, t \in \mathcal{T}_2 : 1 < t \leq |\mathcal{T}_2| - 1, \tag{13}$$

$$g_{it}^{\text{ramp},-} = \frac{\Delta p_{i(t-1)}^{-} + \Delta p_{i(t+1)}^{-}}{2}, \quad i \in \mathcal{I}_t, t \in \mathcal{T}_2 : 1 < t \leq |\mathcal{T}_2| - 1. \tag{14}$$

Hence, the level of manual reserves Δp_{it}^{+} and Δp_{it}^{-} in time period t depends on the previous and the subsequent levels.

3. Generating scenarios for the wind power production

In this section, we describe the process of generating values for the stochastic wind power production ω_{nt}^{s} for $n \in \mathcal{N}$, $s \in \mathcal{S}$, and $t \in \mathcal{T}_2$. For this, we assume that we have, at time $t = 0$, access to wind power forecast $\hat{\omega}_{nt}$ for all $t \in \mathcal{T}_2$; this forecast is typically obtained from a third party. The scenario values for wind power production, ω_{nt}^{s}, are then computed as

$$\omega_{nt}^{s} = \hat{\omega}_{nt} + \varepsilon_{nt}^{s}, \tag{15}$$

where ε_{nt}^{s} is the prediction error in period t and scenario s. This implies that we first create the scenario tree for the prediction errors and then combine these with the forecast to get the wind production values; this is illustrated graphically in Fig. 2 on the next page.

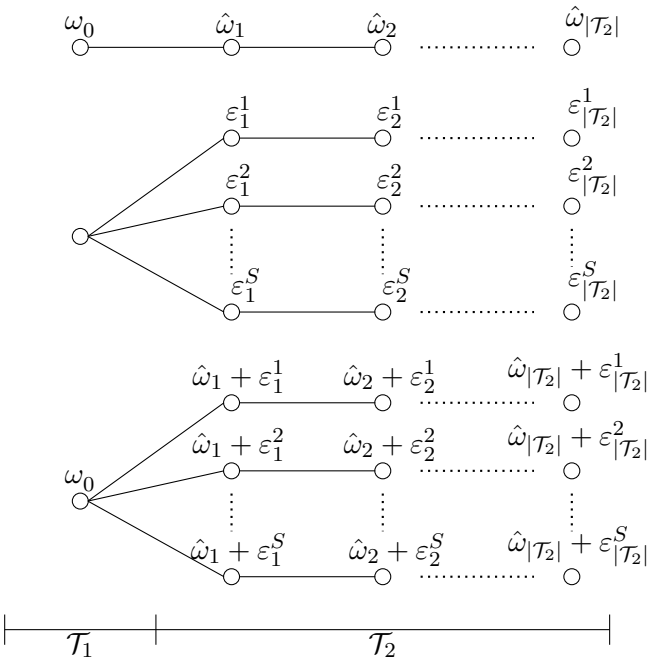

Figure 2: Construction of scenarios. The graph in the top shows an example of a wind power production forecast. The graph in the middle shows an example of scenarios for the prediction error. The graph in the bottom is a combination of the two other graphs and is our scenario tree for the wind power production.

The prediction error is a result of the imprecision of the wind power production forecast. Its statistical properties depend on the length of the forecast and need to be estimated from historical data. For this purpose, we assume that we have access to historical data for both the production and the forecasts for all the forecast lengths Δt used in the model: $\Delta t = \tau\, t$ with $t \in \mathcal{T}_2 = \{1, \ldots, T/\tau\}$. We use a tilde to distinguish the historical data from the model parameters, so $\tilde{\omega}_{n,t}$ denotes the historical wind production at some time $t < 0$, $\tilde{\omega}_{n,t+\Delta t|t}$ stands for the forecast for time $t + \Delta t$ made at time t, and $\tilde{\varepsilon}_{n,t+\Delta t|t}$ is the error of this forecast, i.e.

$$\tilde{\varepsilon}_{n,t+\Delta t|t} = \tilde{\omega}_{n,t+\Delta t|t} - \tilde{\omega}_{n,t+\Delta t}\,.$$

Once we have computed the historical errors $\tilde{\varepsilon}_{n,t+\Delta t|t}$, we can treat them as data series for each n and Δt. Hence, we have a historical data set with dimension $|\mathcal{N}| \times |\mathcal{T}_2|$ for which we want to generate scenarios. Before we delve into the details about how we generate these scenarios, we need to explain how we use the generated values. Since each Δt is a separate data series, we only need to generate values one period ahead. To explain why, let us denote the generated values by $\bar{\varepsilon}^s_{n,\Delta t}$. In the model, on the other hand, we need $\varepsilon^s_{nt} = \bar{\varepsilon}^s_{n,\tau\, t}$, used in (15) to compute the wind production values $\hat{\omega}_{nt}$. This way, we transform scenarios for $|\mathcal{N}| \times |\mathcal{T}_2|$ variables one period ahead into scenarios for $|\mathcal{N}|$ variables $|\mathcal{T}_2|$ periods ahead. This implies, that if $\bar{\varepsilon}^s_{n,\tau\, t}$ correctly captures the $|\mathcal{N}| \times |\mathcal{T}_2|$-dimensional distribution, then ε^s_{nt} will correctly describe not only the dependencies between nodes within each period, but also inter-temporal dependencies such as autocorrelations.

To achieve this, we generate the scenarios using an algorithm from Kaut (2014). This method generates scenarios that try to replicate a specified multivariate distribution; in our case provided by the historical data for forecast errors $\tilde{\varepsilon}_{n,t+\Delta t|t}$. It does so by matching all the univariate distribution functions plus the bivariate *copulas* of all the variable pairs. For the purpose of this paper, a copula can be thought of as a generalisation of the linear correlation, which can fully describe the dependence between stochastic variables – unlike correlations that only capture linear dependencies. See Nelsen (1998) for more information about copulas, and Kaut and Wallace (2011) for a discussion about their use in scenario generation.

With $|\mathcal{N}| \times |\mathcal{T}_2|$ variables, matching copulas for all the $|\mathcal{N}| \times |\mathcal{T}_2|\, \big(|\mathcal{N}| \times |\mathcal{T}_2| - 1\big)\, /\, 2$ variable pairs becomes impractical. By trying to match copulas for so many pairs, the approximation error can be expected to be significant, especially since we can only solve the model with a couple of hundreds scenarios for realistic instances. For this reason, we concentrate only on the most important pairs of variables: for each forecast length Δt, we match the copulas between all the locations/nodes n, and for each node n, we match the copulas between forecasts of similar length, specifically for $0 < \Delta t_2 - \Delta t_1 \leq U\, \tau$. There, $U \geq 1$ is a case-dependent constant, whose value has to be adjusted to the data and also the generated number of scenarios. This reduces the number of bivariate copulas to

$$|\mathcal{T}_2| \times \frac{|\mathcal{N}| \times (|\mathcal{N}| - 1)}{2} + |\mathcal{N}| \times \sum_{l=1}^{U} (|\mathcal{T}_2| - l)\,, \tag{16}$$

a reduction by the factor of more than $T/(1 + 2U/N)$. Naturally, there is a price to pay for this reduction: when we do not specify the dependence between a given pair of variables, it

does not mean that the two variables become independent. It simply means that the algorithm does not have any control over the dependence, except for the constraints implied by the other pairs. For this reason, we need to check the quality of the scenario-generation procedure and its suitability for our optimisation model prior to using it on real data. In our case, these checks indicate that the scenarios-generation procedure performs satisfactorily, as shown in Section 4.2.1.

4. Real-world problem

To investigate the usefulness of the model, we apply it on realistic data from Denmark. We look at two areas, Denmark West and Denmark East, and optimise the use of reserves during four weeks in 2012: a week in January, a week in April, a week in July, and finally, a week in October. We apply the model in a rolling horizon manner where we solve the model with a two hour time horizon every hour. The two hour time horizon is chosen to avoid undesired end effects. We will use the result for the first hour and disregard the result from the second hour, since the second hour will be re-optimised in the subsequent run of the model. The initialisation of each run is based on the state of the last optimised hour that is not disregarded. By utilising rolling horizon, we can take updated information about the system into consideration, and in our case, we get updated wind power production forecasts every hour. Our test instances each cover a week, and thereby they each consist of 168 hours. However, we will only report of 167 hours, since we use the first hour of each case for initialisation. The time resolution of the model, meaning each time interval $]\tau(t-1), \tau t]$, $t \in \mathcal{T}_2$, will represent five minutes.

In each of the four cases, we will compare the cost of balancing the system when having scenarios for the wind power prediction error to the cost of balancing the system when assuming the prediction error to be zero, i.e. to the deterministic case. We investigate how the solution differs in the two cases. Furthermore, in order to show that it makes sense to predict the imbalances in the system and be proactive, we calculate the cost of balancing the system in each of the four weeks by only using automatic reserves. Finally, we investigate what the cost in the four weeks would have been if we were able to predict the actual wind power production, i.e. in the case of perfect foresight. The solution of perfect foresight is a lower bound on the actual cost of balancing the system, which the stochastic solution will never be able to match, but it indicates how far we are from the perfect solution.

We run the model on a computer with an Intel Core 2.30GHz processor and 4 GB RAM. The model is implemented in the 64 bit GAMS framework version 24.2.3 for Windows using the CPLEX 12.6 solver.

4.1. Data

We get unit commitment data from the unit commitment model, Sivael, used by the Danish transmission system operator, Energinet.dk. Real data for the Danish system in 2012 are given as input to the unit commitment model. Afterwards, we use an intra-hour model, SimBa from Energinet.dk, to convert the hourly output from the unit commitment model into a time resolution of five minutes. A description of SimBa can be found in Hansen et al. (2011).

Table 1: Aggregated information about the system for four different weeks in year 2012 used as input to our model. The numbers represent the mean (standard deviation) of the 2016 time periods in the optimisation period, and hence is calculated in MWh/12. Note, capacity is showed in MW and day-ahead forecasts in MWh.

	All areas – 2012 cases			
	January	April	July	October
Demand (MWh/12)	4520(863)	3940(644)	3537 (625)	3976(731)
Conv. prod. (MWh/12)	3363(527)	2571(890)	940 (524)	2342(763)
Online capacity (MW)	5634(249)	5299(337)	3188(1289)	5205(331)
Wind power prod. forecast DA (MWh)	2054(836)	1005(668)	949 (488)	894(791)
Wind power prod. forecast HA (MWh/12)	1958(812)	999(662)	927 (529)	927(785)
Wind power prod. (MWh/12)	1914(811)	996(660)	921 (526)	934(786)
Installed wind capacity (MW)	3926	3969	4025	4038
Import (MWh/12)	931(637)	1811(637)	2322 (443)	1750(801)
Export (MWh/12)	1698(584)	1478(512)	608 (250)	943(748)

Aggregated overall information about demand, conventional production, conventional capacity, wind power production forecasts, actual wind power production, installed capacity, import, and export can be found in Table 1. *Online capacity* is conventional capacity disposal for the market, meaning started up capacity where some of it is already committed by the unit commitment model, the rest of the capacity can be used as reserves for additional electricity production in our model. *Wind power prod. forecast DA* is the forecast made to clear the day-ahead market used in the unit commitment model, where the *wind power prod. forecast HA* is the updated wind power production forecast used in our model. The updated wind power forecasts used are made just before the hour of operation.

In order to resemble real life balancing in the Nordic countries, we follow present market rules and let the ramping period, $\tau^{\max}$, for import, export, and conventional production units be 15 minutes. Having a time resolution of five minutes implies $\tau^{\max} = 3$. Once a generating conventional unit has been re-dispatched, the unit commits to the change in 30 minutes, i.e $\tau^{\text{res}} = 6$. Finally, the unit is guaranteed to have a re-dispatch amount greater than 10 MWh/12, i.e. $G_i^{\min} = 10$ for all $i \in \mathcal{I}$.

The costs of manual reserves are the individual marginal costs of the generating units altered with the parameter γ. The level of marginal costs of the generating units are within the range €2.27-205.73, where γ is set to 0.1 to represent the additional stress imposed on the unit. Recall, that for up-regulating cost the marginal cost of a unit is multiplied by $1 + \gamma$, where for down-regulating cost the marginal cost of a unit is multiplied by $1 - \gamma$.

In practice, the costs for automatic reserves are not known when optimising and activating manual reserves for the next hour. To run our model, we need to estimate a fixed number for the cost of the automatic reserves, and hence we base the level on historical data from 2012. We let the 95% fractile for the historical cost of manually activating additional electricity in the balancing market be the cost for the automatic reserves when additional electricity is activated. Likewise, we let the 5% fractile for the historical cost in the balancing market of

manually deactivating power be the cost for the automatic reserves in the case of deactivation of power. Hence, in our cases, we will assume the cost of activating automatic reserve power to be €75 and the cost of deactivating automatic reserve power to be €10.

4.2. Scenarios for the wind power production

The wind power production scenarios are generated as described in Section 3. Data input to the procedure comes from historical data for the wind power production in Denmark during 2012. The data consists of information about the installed capacity, the actual wind power production, the forecasts made day-ahead and the updated forecasts made just before the hour of operation where the system had to be balanced. Subsequently, we have calculated the historical prediction errors normalised with installed capacity, which is the actual input to the scenario generation procedure. The time resolution of all these time series is five minutes.

Our data analysis of the historical wind data shows a significant difference in the prediction errors between onshore and offshore wind power production, as documented in Fig. 7 and Fig. 8 in Appendix A on page 25. For this reason, we separate the onshore and offshore wind power production in both the studied regions, so we end up with four locations ($N = 4$). Since we solve the model for two hours ahead with five minute steps, we have $T = 120$, $\tau = 5$, and $|\mathcal{T}_2| = T/\tau = 24$. As a result, the model has $N \times |\mathcal{T}_2| = 96$ random variables.

It follows that there are 4560 bivariate copulas to match – too many to get a good match, especially since we can solve the model with a couple of hundreds of scenarios at most. We therefore only match a subset of the copulas as discussed in Section 3. After studying the data, we have decided to use $U = 2$, i.e. to model dependencies between forecast errors with forecasts lengths that differ by two periods at most. Using (16), we see that this reduces the number of copulas to 324; a far more manageable amount.

In order to construct the scenarios, we need exogenous given wind power forecasts, see Fig. 2 on page 10. For this, we use the historical updated wind power forecasts from 2012.

Fig. 3 on the next page shows two graphs. The graph on the left shows 50 scenarios generated by the described scenario generation method. As expected for a short-time forecast, most of the scenarios lie around the forecast (the gray line) with some extreme scenarios farther apart. In most cases, also the actual wind production lies within the range of the scenarios. In rare occasions, however, the forecast is wrong from the start, so the actual wind production will be outside of the range covered by the scenarios, especially at the start of the horizon. This is illustrated by the graph to the right.

The graph in Fig. 4 on the following page shows 50 scenarios for a whole week. Since the model is re-optimised every hour when new scenarios are generated, the scenarios will be close to the new updated forecast every hour, whereafter they will spread out and gather again in the beginning of the next hour.

4.2.1. In-sample and out-of-sample stability tests

Stability and high accuracy of the scenario generation procedure are important to ensure consistency and high quality of the solutions coming from the intra-hour model. In-sample and out-of-sample stability tests, as described in Kaut and Wallace (2007), can be used to measure

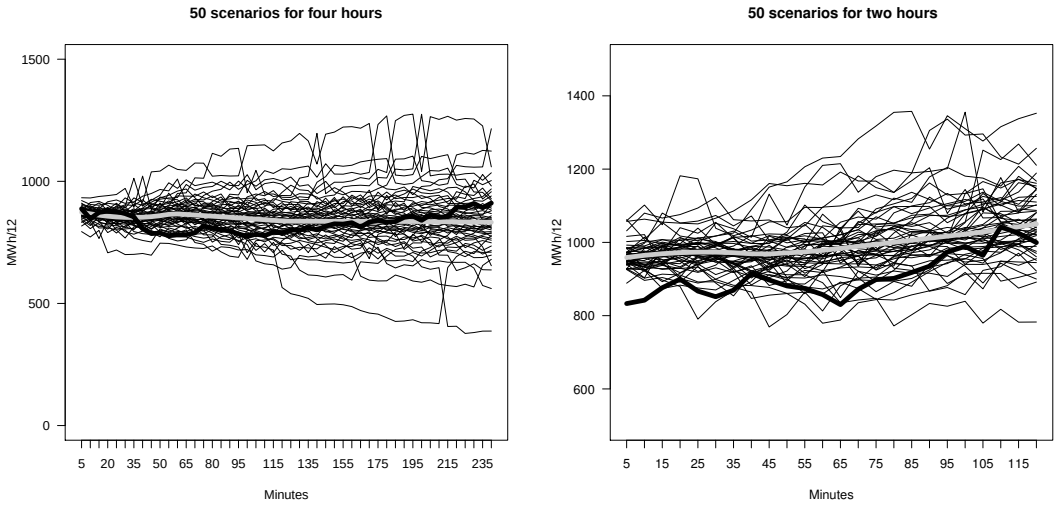

Figure 3: The graph to the left shows 50 generated scenarios for onshore Denmark West from the scenario generation procedure for four hours where the graph to the right shows 50 generated scenarios for two hours during another time period. The gray line shows the wind production forecast, and the thick black line shows the actual wind power production.

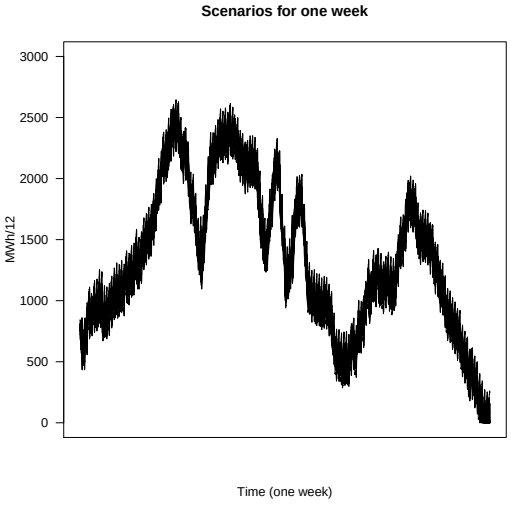

Figure 4: The graph shows 50 generated scenarios for onshore Denmark West for a whole week.

the quality of the scenario generation procedure in relation to the model. According to King et al. (2012), there are at least two ways to perform these tests. Which tests to use depends on the scenario generation procedure itself which will be explained below.

For in-sample stability, it is important to ensure that the objective function value of the model is approximately the same each time it is run on the same data. There are at least to ways to perform tests for in-sample stability. First, if the scenario generation procedure generates different scenario trees, it is important to test if different trees of the same size generate the same objective function value. Second, if the scenario generation procedure generates the same tree each time, then trees of different sizes have to be investigated. In order to have in-sample stability in the latter of the two cases, the objective function value should not change when changing the tree size with a small amount.

For out-of-sample stability, the value of implementing the first-stage variables and optimise the second-stage variables with respect to the true distribution of the random variables should not change between different runs. Again, when investigating the stability, the stochasticity of the scenario generation procedure has to be taken into account as described under in-sample stability.

Another important factor to investigate is the bias of the model. If the objective function value of the model when it is optimised over the entire distribution of the random variables is different from the objective function values given by the model when optimised over the scenario trees, then the scenarios do not represent the underlying distribution well enough.

The copula-based method we use for generating the scenarios for the error terms is somewhere between the two cases described above: since it is probabilistic repeated runs with the same input parameters, it typically results in very few distinct trees. For this reason, we combine the two approaches to stability and run the intra-hour model 10 times for the following number of scenarios: 1, 5, 10, 20, 30, 50, 75, 100, 125, 150, 175, and 200. However, if stability is achieved before we have investigated all the tree sizes, we stop. The case with 1 scenario is the deterministic variant of the model.

For the stability tests, we report the following values: (V1) is the in-sample objective value, i.e. the objective value of the scenario-based model. The out-of-sample value (V2) is computed by fixing the first-stage decisions and re-optimising using all the historical data as our scenarios. In order to measure the bias, we also calculate the value (V3) for the objective value of the model optimised over all the historical data. Note, that we are able to calculate (V3) only because we investigate these two small cases. It will be too time consuming to apply the model on the full cases with all the historical data for the prediction errors. In the stability tests, we should optimally see both (V1) and (V2) stabilising and approaching (V3) with the increasing number of scenarios.

We run the model with a two hour time horizon. Due to the complexity of the model, we have chosen two hours in January and two hours in July as representative cases for the full instances. The January two-hour case is difficult for the model to solve, while the July two-hour case is solved easily. Since the model is normally run with rolling horizon where the last hour of a model run is re-optimised in the subsequent run of the model, the output function of the model is only implemented for the first hour. Hence, we report the costs in these test only for the first hour.

Fig. 5 on the next page shows the results of the tests. The figure shows that, for a given size

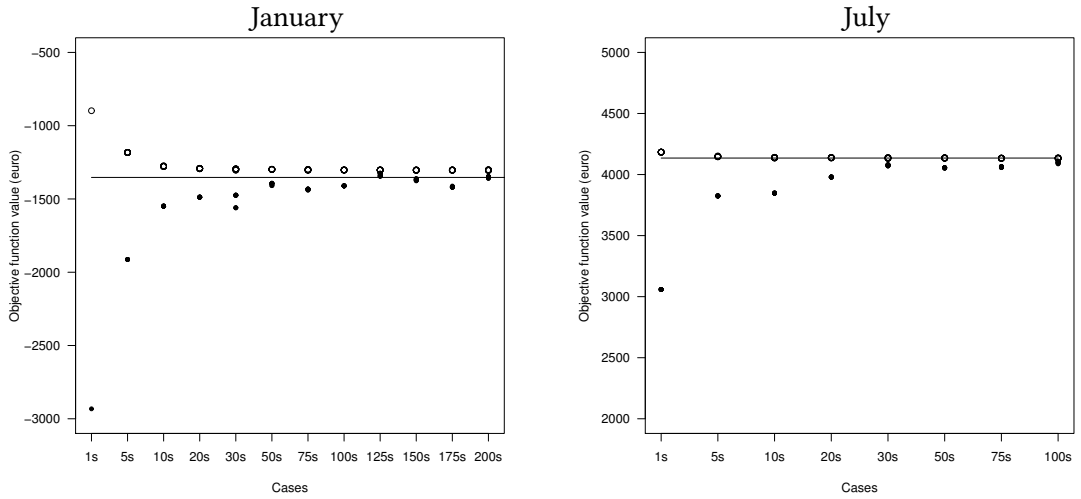

Figure 5: In this figure, we see two graphs showing the objective function value for our in- and out-of-sample stability tests for the two studies months. • represents values from (V1), ○ represents values from (V2), and the black line represents values from (V3).

of the scenario tree, the scenario generation procedure is indeed stable: for most of the tree sizes, we only see one dot in the figure for each of the measurements (V1) and (V2). However, running the model with different tree sizes shows some instability. Looking at the graph to the left in Fig. 5, we can see that the values improve fast when including up until 50 scenarios. After 50 scenarios, the values are approaching each other very slowly and the values of the three different measurements lie relatively close. However, with 200 scenarios, the values of the three measurements are still not exactly the same. Looking at the graph on the right, we see that the three measurements give approximately the same value already when including 30 scenarios.

We choose to run our full test instances with 50 scenarios. The tests show that the objective function value is reasonably stable around 50 scenarios, while the solution time is still manageable: it would be too time consuming to run the full tests with the 200 scenarios that are required for significantly better stability.

4.3. Results

In this section, we will present the obtained results. We will present results from four different versions of the model presented in Section 2. The first version is the stochastic model, where we apply the scenario generation procedure described in Section 3 to make 50 scenarios for the wind power production for each of the individual hours in the test instances. The second version is the deterministic model, where we only have one scenario for the wind power production and that is the expected value, i.e. where the expectation of the error-term is zero. The third version is the case of perfect foresight, where we also only have one scenario for the wind power production, but this scenario is the actual realised wind power production. The fourth and final version is also the stochastic model, but with an extra constraint forcing the manual reserves to zero, such that only automatic reserves are utilised.

Table 2: Average objective function values and actual values in € and CPU time of the cases. The total CPU time is displayed hours first and then additional minutes (h:m).

		Objective value		Actual cost		CPU time		
Case	Model	Average	Std.	Average	Std.	< 1 min.	> 10 min.	Total
January	Stochastic	2751	16 862	4765	17 526	76.0%	4.2%	3:48
	Deterministic	1465	16 892	5269	17 364	73.1%	9.6%	6:34
	Perfect foresight	2123	17 225	2123	17 225	68.8%	9.0%	6:51
April	Stochastic	6844	14 069	7338	13 755	86.2%	2.4%	2:25
	Deterministic	5598	14 144	7639	13 644	85.6%	6.6%	4:13
	Perfect foresight	5643	13 774	5643	13 774	87.4%	4.2%	3:23
July	Stochastic	−82	7274	405	7543	99.4%	0.0%	0:33
	Deterministic	−1392	7052	727	7577	97.0%	0.0%	0:38
	Perfect foresight	−1383	7087	−1383	7087	97.6%	0.0%	0:38
October	Stochastic	−3442	8102	−3276	8179	92.2%	0.6%	1:27
	Deterministic	−4883	8089	−2893	8233	86.8%	3.6%	3:04
	Perfect foresight	−5072	8151	−5072	8151	86.8%	0.6%	2:12

Table 2 displays the average objective function value (which we will call average expected cost) and its standard deviation over the individual hours in the investigated weeks for each of three models: the stochastic, the deterministic, and the case of perfect foresight. The high standard deviation indicates significant variability in the costs between individual hours. This is further supported by Fig. 6 on the next page, which shows the expected hourly cost for the deterministic January case together with the expected imbalance.

Comparing the objective function values of the stochastic and deterministic models, we can see that the the stochastic solutions have higher expected costs; this is to be expected, since the stochastic model needs to hedge against uncertainty. Table 2 also displays the actual (real) cost of implementing the solution value of the first-stage decision variables. Here, the difference is reversed: the deterministic solutions cannot cope with the uncertainty and end up being more expensive than the stochastic ones on average. We can thus conclude that for the investigated problem, it is beneficial (on average) to use a stochastic model instead of a deterministic model.

Looking at the running times of the model (also displayed in Table 2), we see that for most of the hours, the model is quite fast: between 68.8% and 99.4% of the individual hours in each ccase are solved within a minute. However, a few of the instances take considerably more time: between 0% and 9.6% of the instances take more than ten minutes (and often even much more) to solve. For the numbers displayed in Table 2 the optimisation of an individual hour was stopped after 1000 sec., which happened in 1.8% of the cases. For those hours not solved to optimality, the gap was 0.6% at most.

Analysing the difficult instances, we note that these represent hours with large changes in the supply of power over a very short time, or hours, where the overall production level is close to the overall minimum or maximum capacity level. Looking at the overall running time for each of the different cases for the four weeks, we see that the stochastic model is solved faster than the deterministic model which is not what we expected to see. We also see that there

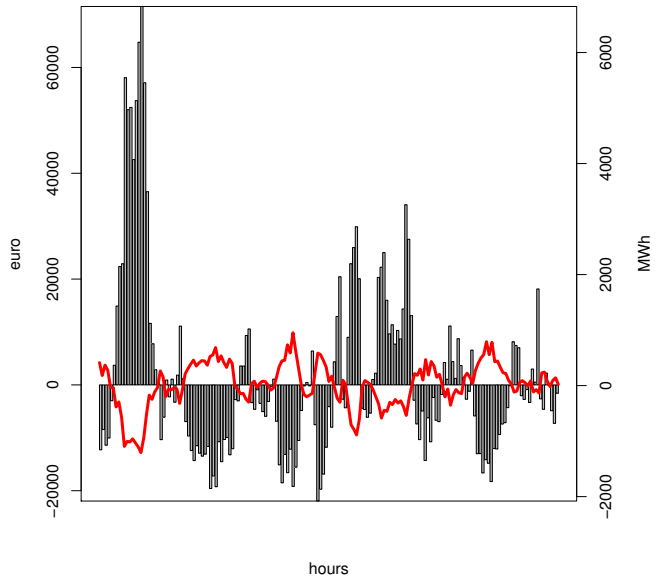

Figure 6: The columns show the expected cost in € for each hour in the deterministic January case. The cost is shown on the y-axis to the left. The line displays the expected imbalance in MWh in each of the corresponding hours of the case. The imbalances relate to the y-axis on the right.

are more of the individual hours that require a long running time in order to find the optimal solution in the deterministic model compared to the stochastic model. In order to explain this, we will first point out that the second-stages of the stochastic model are solved very fast. Second, in Table 3, we see that the stochastic solution on average activates more additional power and deactivate less than the deterministic solution. In all four cases, the gap between the aggregated planned production level and the overall minimum capacity level is smaller than the gap between the maximum production level and the aggregated planned production level. This means that on the short-term horizon, we can activate more power than we can deactivate. Since cases where the production level is close to the capacity limits are difficult to solve, an explanation for the longer running time of the deterministic cases could be that the production level comes close to the minimum capacity level.

Table 3: The average difference in manually activated or deactivated power between the stochastic and the deterministic solution (stochastic - deterministic). The numbers are displayed in MWh/12.

Case	Average up	Average down
January	5.64	-20.37
April	11.99	-12.32
July	11.09	-9.08
October	29.61	-21.21

Table 4 on the following page shows the aggregated total cost for the whole week given by the stochastic solution, the deterministic solution, and in case of perfect foresight for each of the four test instances. The results in Table 4 support the results in Table 2 and show that in all cases, the total cost given by the objective function of the stochastic solution is higher than the total cost given by the objective function of the deterministic solution. However, implementing the deterministic solution compared to implementing the stochastic solution entails a higher total actual cost in all of the four weeks. Looking at Table 5 on the next page, we see that the actual cost of the stochastic solution is actually smaller than the actual cost given by the deterministic solution in 62% - 77% of the individual hours in the four weeks.

As pointed out earlier, in the stochastic solution we manually activate more additional power and deactivate less than in the deterministic solution. It can be seen in Table 4 that the stochastic solution also deactivates more automatic reserve power than in the deterministic case, and it activates less automatic reserve power. Since it is cheaper to activate manual reserve power than automatic reserve power, the stochastic solution builds in a buffer by assuring a higher level of produced power before the hour of operation. If there is no need for the additional power, it will be deactivated by the automatic reserves.

Now, one could think that incorporating this buffer could be rather expensive and that it could be beneficial not to be proactive and just leave all the imbalances to the automatic reserves. However, when looking at Table 6 on page 22, we see that the actual cost of such an approach is very expensive. Hence, it is better to be proactive even though it can occasionally result in activation of manual reserves which is deactivated by automatic reserves when the uncertainty is revealed.

If there had been no uncertainty in the wind power production, we would have had the

cost given by the solution of perfect foresight. If we could predict the wind power production precisely, it would result in huge savings. For July, it is more than four times the cost of the stochastic solution, and else it is between 23% and 55%.

Table 4: Weekly costs of operating the system. All numbers listed are in €.

Case	Strategy		Man. act.	Man. deact.	Auto. act.	Auto. deact.	Total
January	Stochastic	Expected	1 232 805	−1 372 805	709 147	−109 734	459 413
		Actual			1 042 456	−106 663	795 793
	Deterministic	Expected	1 222 213	−1 460 396	518 206	−35 329	244 694
		Actual			1 202 638	−84 587	879 868
	Perfect foresight		1 269 633	−1 392 438	510 245	−32 868	354 572
April	Stochastic	Expected	2 431 796	−2 180 726	1 013 361	−121 524	1 142 907
		Actual			1 107 806	−133 420	1 225 456
	Deterministic	Expected	2 425 102	−2 236 951	796 819	−50 079	934 891
		Actual			1 191 575	−104 000	1 275 726
	Perfect foresight		2 397 138	−2 228 160	823 970	−50 538	942 410
July	Stochastic	Expected	627 105	−671 029	199 857	−169 679	−13 746
		Actual			286 194	−174 569	67 701
	Deterministic	Expected	590 006	−716 442	4328	−110 351	−232 459
		Actual			404 581	−156 676	121 469
	Perfect foresight		576 937	−707 088	2329	−103 125	−230 947
October	Stochastic	Expected	758 591	−1 419 053	226 467	−140 882	−574 877
		Actual			271 469	−158 158	−547 151
	Deterministic	Expected	693 241	−1 504 818	23 525	−27 475	−815 527
		Actual			421 750	−93 332	−483 159
	Perfect foresight		669 776	−1 509 467	21 028	−28 356	−847 019

Table 5: Comparison of the solutions given by the stochastic model and the deterministic model. For each of the two models, it is shown in how many of the individual hours the model found a solution with lowest actual cost.

Case	Deterministic best	Stochastic best
January	23%	77%
April	37%	63%
July	34%	66%
October	38%	62%

5. Conclusion

In this paper, we have presented a stochastic model for the short-term balancing problem between demand and consumption of electricity. We have made scenarios for the wind power prediction error by a copula-based heuristic that captures the dependency between all the wind

Table 6: Weekly actual costs of operating the system with only automatic reserves. All numbers listed are in €.

Case	Total cost
January	2 368 144
April	3 838 005
July	809 076
October	462 443

variables but also the dependency of the errors of the individual wind variables through time.

The results show that the stochastic model is superior to the deterministic model when looking at the actual cost of the solutions. The stochastic model builds in a buffer of additional electricity by activating more manual reserve power than the deterministic model. It does so since it is cheaper to activate the manual reserves than the automatic reserves, and if there is no need for the additional power, it is deactivated by the automatic reserves.

The results also show that it is a good idea to be proactive and activate manual reserves before the actual imbalances occur. It will be much more expensive to only let the automatic reserves handle the imbalances.

Acknowledgments

The authors gratefully appreciate all the support they have received from Energinet.dk in getting data and lending the models Sivael and Simba throughout this project. Furthermore, the authors appreciate the work Stephan Wllner at Energinet.dk has made to make Simba work together with our model OPTIBA. Jeanne Andersen acknowledges support through the CFEM project.

References

Andersen, J., D. M. Heide-Jørgensen, N. K. Detlefsen, and T. K. Boomsma (2014). Short-term balancing of supply and demand in an electricity system: Forecasting and scheduling. Submitted to Annals of Operations Research.

Bludszuweit, H., J. Dominguez-Navarro, and A. Llombart (2008, Aug). Statistical analysis of wind power forecast error. *Power Systems, IEEE Transactions on 23*(3), 983–991.

Bouffard, F. and F. Galiana (2008, May). Stochastic security for operations planning with significant wind power generation. *Power Systems, IEEE Transactions on 23*(2), 306–316.

Bruninx, K. and E. Delarue (2014, July). A statistical description of the error on wind power forecasts for probabilistic reserve sizing. *Sustainable Energy, IEEE Transactions on 5*(3), 995–1002.

Delikaraoglou, S., K. Heussen, and P. Pinson (2014). Operational strategies for predictive dispatch of control reserves in view of stochastic generation. In *Power Systems Computation Conference (PSCC), 2014*.

Doherty, R. and M. O'Malley (2005, May). A new approach to quantify reserve demand in systems with significant installed wind capacity. *Power Systems, IEEE Transactions on 20*(2), 587–595.

Ela, E. and M. O'Malley (2012, Aug). Studying the variability and uncertainty impacts of variable generation at multiple timescales. *Power Systems, IEEE Transactions on 27*(3), 1324–1333.

Hansen, A., A. Orths, K. Falk, and N. K. Detlefsen (2011). Danish fossil independent energy system 2050 – from strategic investigations to intra-hour simulation of balancing issues. In *10th Internation Workshop on Large-Scale Integration of Wind Power into Power Systems, Aarhus*.

Hodge, B. and M. Milligan (2011, July). Wind power forecasting error distributions over multiple timescales. In *Power and Energy Society General Meeting, 2011 IEEE*, pp. 1–8.

Kaut, M. (2014). A copula-based heuristic for scenario generation. *Computational Management Science 11*(4), 503–516.

Kaut, M. and S. W. Wallace (2007). Evaluation of scenario-generation methods for stochastic programming. *Pacific Journal of Optimization 3*(2), 257–271.

Kaut, M. and S. W. Wallace (2011). Shape-based scenario generation using copulas. *Computational Management Science 8*(1–2), 181–199.

King, A. J., S. W. Wallace, and M. Kaut (2012). *Scenario-Tree Generation*, Chapter 4, pp. 77–102. Springer Series in Operations Research and Financial Engineering. Springer New York.

Lange, M. (2005). On the uncertainty of wind power predictions - analysis of the forecast accuracy and statistical distribution of errors. *Journal of Solar Energy Engineering 127*(2), 177–184.

Lindgren, E. and L. Söder (2008). Minimizing regulation costs in multi-area systems with uncertain wind power forecasts. *Wind Energy 11*(1), 97–108.

Litong-Palima, M., N. A. Cutululis, N. Detlefsen, and P. Sørensen (2012). Wind-induced day-ahead and hour-ahead imbalances in a power system with a significant wind mix: Simulations in the danish experience. In *European Wind Energy Conference & Exhibition, European Wind Energy Association (EWEA)*.

Ma, X.-Y., Y.-Z. Sun, and H.-L. Fang (2013, Oct). Scenario generation of wind power based on statistical uncertainty and variability. *Sustainable Energy, IEEE Transactions on 4*(4), 894–904.

Matevosyan, J. and L. Söder (2006, Aug). Minimization of imbalance cost trading wind power on the short-term power market. *Power Systems, IEEE Transactions on 21*(3), 1396–1404.

Menemenlis, N., M. Huneault, and A. Robitaille (2012, Oct). Computation of dynamic operating balancing reserve for wind power integration for the time-horizon 1-48 hours. *Sustainable Energy, IEEE Transactions on 3*(4), 692–702.

Nelsen, R. B. (1998). *An Introduction to Copulas*. New York: Springer-Verlag.

Papavasiliou, A. and S. S. Oren (2013). Multiarea stochastic unit commitment for high wind penetration in a transmission constrained network. *Operations Research 61*(3), 578–592.

Pappala, V., I. Erlich, K. Rohrig, and J. Dobschinski (2009, May). A stochastic model for the optimal operation of a wind-thermal power system. *Power Systems, IEEE Transactions on 24*(2), 940–950.

Pinson, P., H. Madsen, H. A. Nielsen, G. Papaefthymiou, and B. Klöckl (2009). From probabilistic forecasts to statistical scenarios of short-term wind power production. *Wind Energy 12*(1), 51–62.

Söder, L. (2004, Sept). Simulation of wind speed forecast errors for operation planning of multiarea power systems. In *Probabilistic Methods Applied to Power Systems, 2004 International Conference on*, pp. 723–728.

Tewari, S., C. Geyer, and N. Mohan (2011, Nov). A statistical model for wind power forecast error and its application to the estimation of penalties in liberalized markets. *Power Systems, IEEE Transactions on 26*(4), 2031–2039.

Weber, C., P. Meibom, R. Barth, and H. Brand (2009). Wilmar: A stochastic programming tool to analyze the large-scale integration of wind energy. In J. Kallrath, P. Pardalos, S. Rebennack, and M. Scheidt (Eds.), *Optimization in the Energy Industry*, Energy Systems, pp. 437–458. Springer Berlin Heidelberg.

Wu, J., B. Zhang, H. Li, Z. Li, Y. Chen, and X. Miao (2014). Statistical distribution for wind power forecast error and its application to determine optimal size of energy storage system. *International Journal of Electrical Power & Energy Systems 55*, 100–107.

A. Graphs for historical wind data

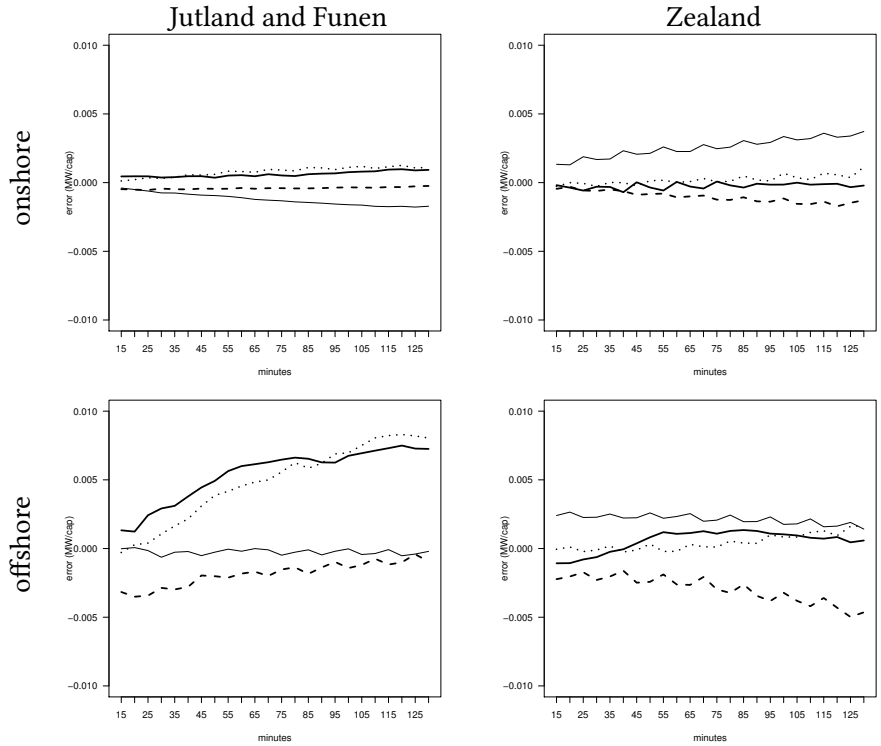

Figure 7: The average of the normalised wind power prediction errors in Denmark recorded in 2012 for each of the four months we investigate. The thin line represents values for January, the thick line represents values for April, the scattered line represents values for July, and the dotted line represents values for October.

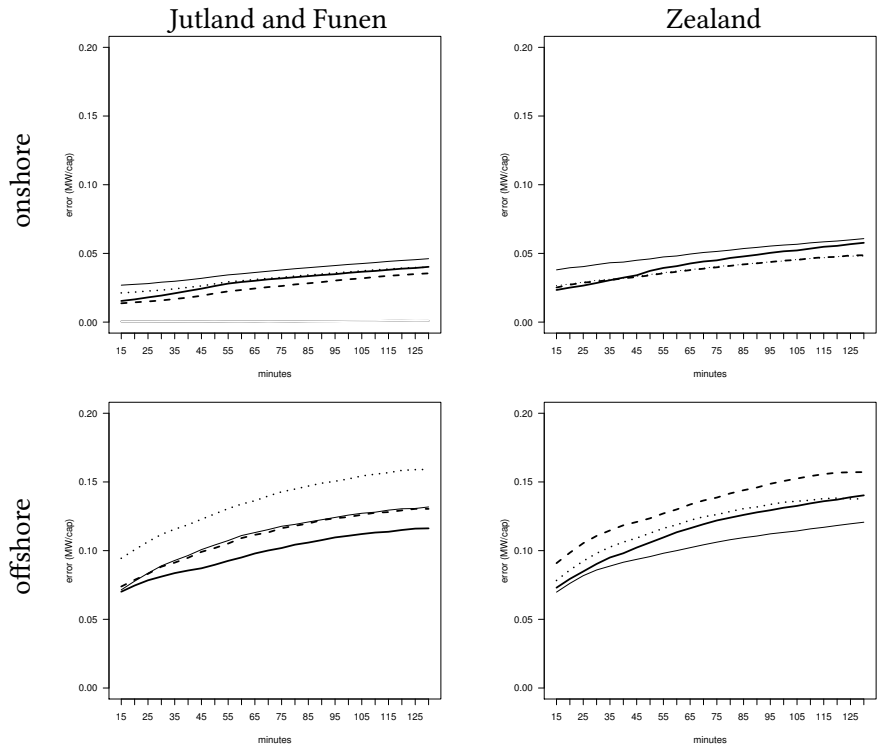

Figure 8: Standard deviation of the normalised wind power prediction errors in Denmark recorded in 2012 for each of the four months we investigate. The thin line represents values for January, the thick line represents values for April, the scattered line represents values for July, and the dotted line represents values for October.